SUPPLEMENTARY MATERIALS

Scoring Molecular Wires Subject to Ultra-Fast Laser Irradiation for Molecular Electronic Devices

Hui Lu[1], Alireza Azizi[2], Xiao Peng Mi[1], Yu Wenjing[1], Yuting Peng[1], Tianlv Xu[1], Herbert Früchtl[3], Tanja van Mourik[3], Steven R. Kirk[*1] and Samantha Jenkins[*1]

[1]*Key Laboratory of Chemical Biology and Traditional Chinese Medicine Research and Key Laboratory of Resource National and Local Joint Engineering Laboratory for New Petro-chemical Materials and Fine Utilization of Resources, College of Chemistry and Chemical Engineering, Hunan Normal University, Changsha, Hunan 410081, China.*
[2]*State Key Laboratory of Powder Metallurgy, School of Materials Science & Engineering, Central South University, Changsha, Hunan 410083, China*
[3]*EaStCHEM School of Chemistry, University of Saint Andrews, North Haugh, St Andrews, Fife KY16 9ST, Scotland, United Kingdom.*

email: steven.kirk@cantab.net
email: samanthajsuman@gmail.com

1. Supplementary Materials S1. Tabulated excitation frequencies ω for excited states and populations of the states of selected laser pulse frequencies of ethene.

2. Supplementary Materials S2. Time variations of the laser pulse frequencies for ethene.

3. Supplementary Materials S3. Distance measures for the C-H *BCP* bond-path.

4. Supplementary Materials S4. The variation of the precession $\mathbb{K}$, $\mathbb{K}'$ along the C1-C2 *BCP* bond-paths.

5. Supplementary Materials S5. Ethene bond-path framework set $\mathbb{B}$ with $\{p, p'\}$ path-packets.

1. Supplementary Materials S1.

Table S1. Excitation frequencies ω for excited states from initial time dependent density functional theory (TDDFT) zero electric field calculations in atomic units (au).

| Electronic State	Excitation frequency ω (a.u)
S_0	0.0000000
S_1	0.2583882
S_2	0.2799563
S_3	0.2816762
S_4	0.2843111
S_5	0.3030937
S_6	0.3126559
S_7	0.3220600
S_8	0.3260951
S_9	0.3380092
S_{10}	0.3529111
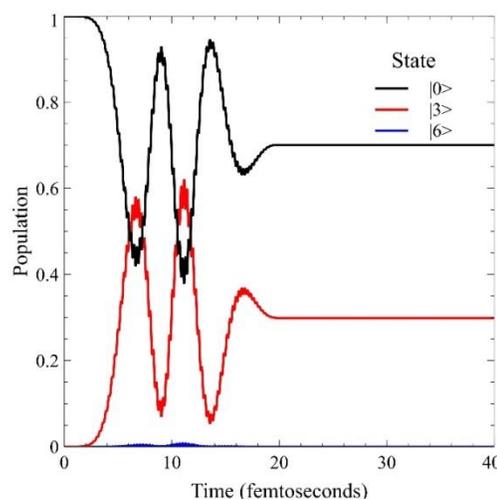
(a)
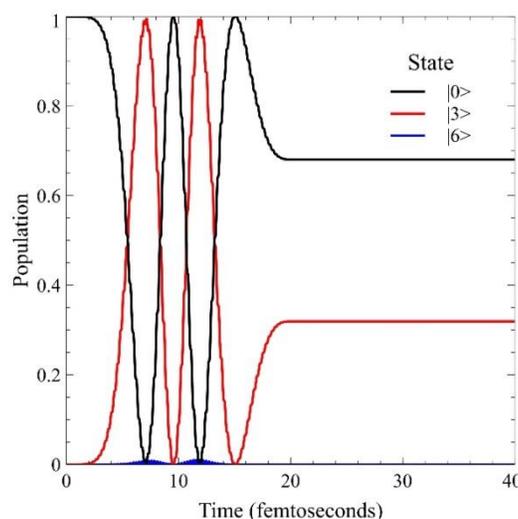
(b)
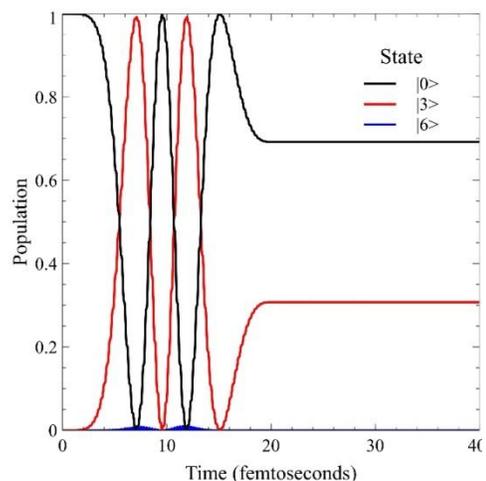
(c)
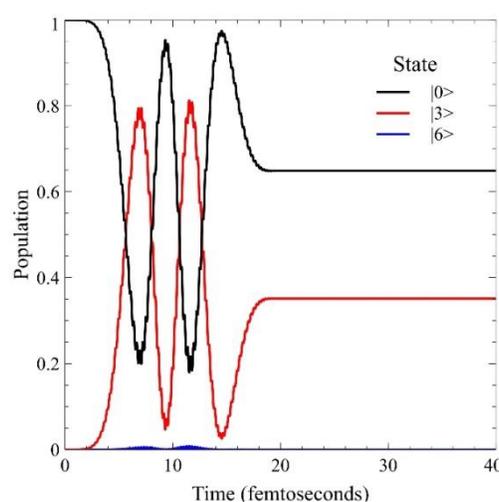
(d)

Figure S1. The variations of population of electronic states, that are non-zero, with time for the laser pulse frequencies 0.26917 au, 0.28081 au, 0.283 au, and 0.290 au are provided in sub-figures **(a)-(d)** respectively.

2. Supplementary Materials S2. Time variations of the laser pulse frequencies for ethene.
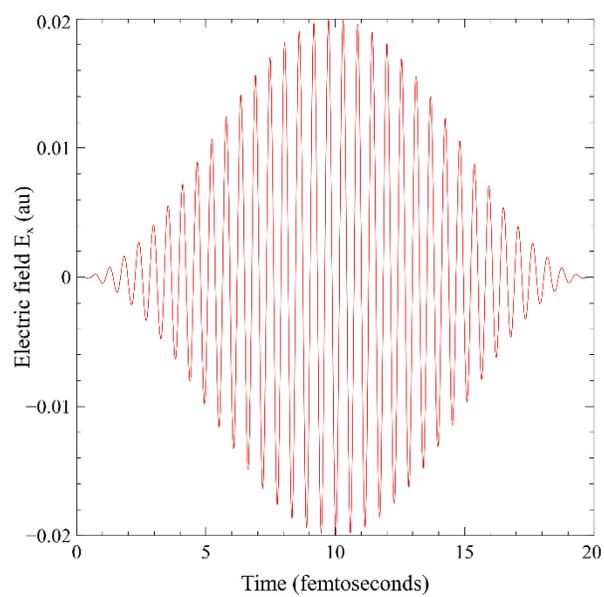

(a)
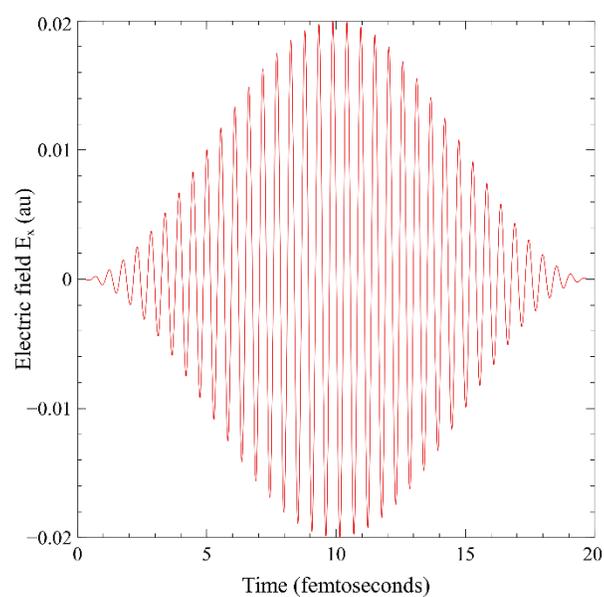
(b)
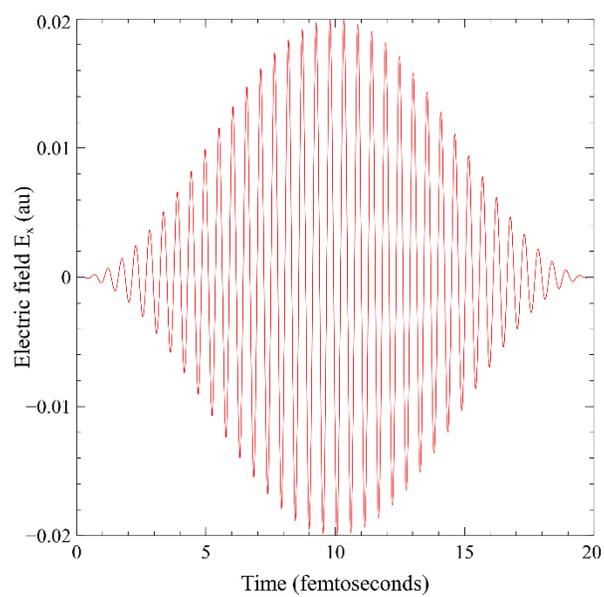
(c)
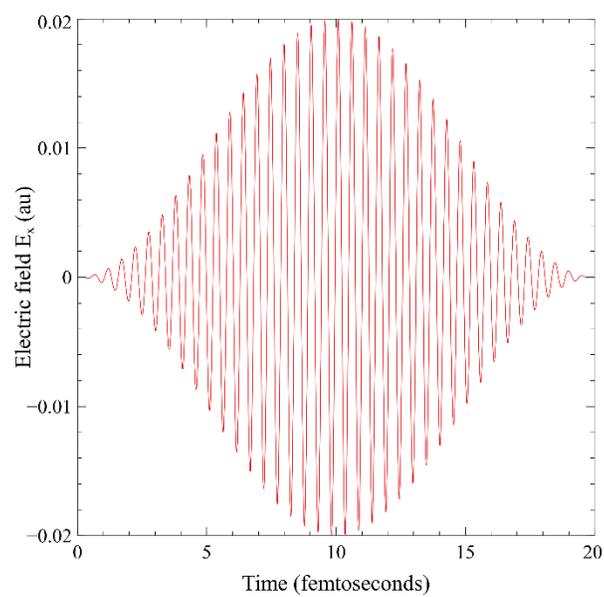
(d)

Figure S2. Time variations of the laser pulse frequencies 0.26917 au, 0.28081 au, 0.283 au, and 0.290 au are provided in sub-figures **(a)-(d)** respectively.

3. Supplementary Materials S3. Distance measures for the C-H *BCP* bond-path.

Table S3. The values of the partial bond-path lengths (BPL) (in a.u.). Each entry for the $\mathbf{E}_x$ is in units of x10^{-4} a.u.

$\omega = 0.26917$ au

Pulse (fs)	±$\mathbf{E}_x$	Index	C1-*BCP*, *BCP*-H4	H5-*BCP*, *BCP*-C2	Δ(C1-*BCP*,*BCP*-H4)	Δ(H5-*BCP*, *BCP*-C2)
5.224	+107.0	0232	1.310, 0.731	0.740, 1.301	0.005, -0.005	0.005, -0.005
4.944	-98.2	0220	1.301, 0.740	0.731, 1.310	-0.005, 0.005	-0.005, 0.005
9.742	+199.6	0433	1.311, 0.730	0.740, 1.301	0.005, -0.005	0.005, -0.005
10.022	-200.0	0445	1.302, 0.739	0.731, 1.310	-0.004, 0.004	-0.005, 0.005
14.821	+105.6	0658	1.309, 0.732	0.738, 1.303	0.003, -0.003	0.003, -0.003
15.101	-96.8	0671	1.302, 0.739	0.731, 1.310	-0.004, 0.004	-0.004, 0.004

After pulse (fs)						
20.0	---	0888	1.303, 0.738	0.732, 1.309	-0.003, 0.003	-0.003, 0.003
40.0	---	1777	1.302, 0.739	0.731, 1.310	-0.004, 0.004	-0.004, 0.004
60.0	---	2665	1.303, 0.738	0.732, 1.309	-0.003, 0.003	-0.003, 0.003
80.0	---	3553	1.304, 0.737	0.733, 1.308	-0.002, 0.002	-0.002, 0.002
100.0	---	4451	1.303, 0.738	0.732, 1.309	-0.003, 0.003	-0.003, 0.003

$\omega = 0.28081$ au

Pulse (fs)	±$\mathbf{E}_x$	Index	C1-*BCP*, *BCP*-H4	H5-*BCP*, *BCP*-C2	Δ(C1-*BCP*, *BCP*-H4)	Δ(H5-*BCP*, *BCP*-C2)
5.011	+100.2	0232	1.306, 0.735	0.735, 1.306	0.000, 0.000	0.000, 0.000
4.741	-91.7	0220	1.305, 0.736	0.734, 1.307	-0.001, 0.001	-0.001, 0.001
9.882	+199.7	0459	1.307, 0.734	0.736, 1.305	0.001, -0.001	0.001, -0.001
10.151	-199.8	0471	1.306, 0.735	0.735, 1.306	0.000, 0.000	0.000, 0.000
14.752	+107.7	0685	1.306, 0.735	0.735, 1.305	0.000, 0.000	0.000, 0.000
15.022	-99.3	0698	1.305, 0.735	0.735, 1.306	0.000, 0.000	0.000, 0.000
20.0	---	0929	1.299, 0.742	0.728, 1.313	-0.007, 0.007	-0.007, 0.007
40.0	---	1857	1.299, 0.742	0.728, 1.313	-0.007, 0.007	-0.007, 0.007
60.0	---	2786	1.300, 0.741	0.730, 1.311	-0.006, 0.005	-0.005, 0.006
80.0	---	3715	1.303, 0.738	0.732, 1.309	-0.003, 0.003	-0.003, 0.003
100.0	---	4643	1.305, 0.736	0.734, 1.307	-0.001, 0.001	-0.001, 0.001

$\omega = 0.283$ au

Pulse (fs)	±$\mathbf{E}_x$	Index	C1-*BCP*, *BCP*-H4	H5-*BCP*, *BCP*-C2	Δ(C1-*BCP*, *BCP*-H4)	Δ(H5-*BCP*, *BCP*-C2)
4.968	+99.0	0233	1.306, 0.735	0.736, 1.305	0.000, 0.000	0.000, 0.000
5.235	-107.4	0245	1.307, 0.734	0.736, 1.305	0.001, -0.001	0.001, -0.001
9.797	+199.6	0459	1.306, 0.735	0.735, 1.306	0.000, 0.000	0.000, 0.000
10.064	-199.6	0471	1.307, 0.734	0.736, 1.305	0.001, -0.001	0.001, -0.001
15.171	+94.6	0710	1.306, 0.735	0.735, 1.306	0.000, 0.000	0.000, 0.000
14.904	-103.0	0698	1.306, 0.735	0.735, 1.305	0.000, 0.000	0.000, 0.000
20.0	---	0936	1.304, 0.737	0.733, 1.308	-0.002, 0.002	-0.002, 0.002
40.0	---	1872	1.307, 0.734	0.736, 1.305	0.001, -0.001	0.001, -0.001
60.0	---	2808	1.309, 0.732	0.738, 1.302	0.004, -0.004	0.003, -0.003
80.0	---	3744	1.312, 0.729	0.741, 1.300	0.006, -0.006	0.006, -0.006
100.0	---	4679	1.312, 0.729	0.741, 1.300	0.006, -0.006	0.006, -0.006

$\omega = 0.290$ au

Pulse (fs)	$\pm E_x$	Index	C1-*BCP*, *BCP*-H4	H5-*BCP*, *BCP*-C2	Δ(C1-*BCP*, *BCP*-H4)	Δ(H5-*BCP*, *BCP*-C2)
4.854	+95.1	0233	1.304, 0.737	0.733, 1.308	-0.002, 0.002	-0.002, 0.002
5.115	-103.4	0246	1.308, 0.733	0.737, 1.304	0.002, -0.002	0.002, -0.002
10.083	+199.6	0484	1.302, 0.739	0.732, 1.309	-0.004, 0.004	-0.004, 0.004
9.823	-199.7	0471	1.310, 0.731	0.739, 1.302	0.004, -0.004	0.004, -0.004
14.802	+106.1	0710	1.303, 0.738	0.733, 1.308	-0.002, 0.002	-0.002, 0.002
15.062	-97.9	0722	1.309, 0.732	0.738, 1.303	0.003, -0.003	0.003, -0.003
20.0	---	0959	1.301, 0.740	0.730, 1.311	-0.005, 0.005	-0.005, 0.005
40.0	---	1918	1.299, 0.741	0.729, 1.312	-0.006, 0.006	-0.006, 0.006
60.0	---	2877	1.299, 0.742	0.728, 1.313	-0.007, 0.007	-0.007, 0.007
80.0	---	3836	1.299, 0.742	0.728, 1.313	-0.007, 0.007	-0.007, 0.007
100.0	---	4795	1.300, 0.741	0.730, 1.311	-0.005, 0.005	-0.005, 0.006

Table S3(b). Values of the Q1 corresponds to the area under the Precession $\mathbb{K}'$ plot in the absence of an electric field from C1 to the *BCP*, Q2 corresponds to the area under the Precession $\mathbb{K}'$ plot from the *BCP* to C2 in atomic units (a.u).

Time (fs)	$\pm E_x$	(Q1,Q2)
0.0	---	(0.743, 0.743)

Table S3(c). Values of the Q1 and Q2 are the areas under the corresponding Precession $\mathbb{K}'$ plots. The laser pulse electric field E_x was directed along the bond-path with units of x10^{-4} a.u, see **Table 1** and **Scheme 1**.

Pulse (fs)	$\omega = 0.2692$ au		$\omega = 0.2808$		$\omega = 0.2830$		$\omega = 0.290$	
	$\pm E_x$	(Q1, Q2)	$\pm E_x$	(Q1, Q2)	$\pm E_x$	(Q1, Q2)	$\pm E_x$	(Q1, Q2)
5.224	+107.0	(0.535, 1.026)	+100.2	(0.648, 0.610)	+99.0	(0.610, 0.648)	+95.1	(0.780, 0.591)
4.944	-98.2	(1.026, 0.554)	-91.7	(0.686, 0.629)	-107.4	(0.572, 0.629)	-103.4	(0.572, 0.743)
9.742	+199.6	(0.572, 1.045)	+199.7	(0.705, 0.780)	+199.6	(0.743, 0.724)	+199.6	(0.950, 0.572)
10.022	-200.0	(1.026, 0.535)	-199.8	(0.705, 0.686)	-199.6	(0.686, 0.743)	-199.7	(0.610, 0.969)
14.821	+105.6	(0.591, 0.894)	+107.7	(0.724, 0.761)	+94.6	(0.761, 0.743)	+106.1	(0.875, 0.648)
15.101	-96.8	(1.026, 0.572)	-99.3	(0.761, 0.724)	-103.0	(0.724, 0.761)	-97.9	(0.648, 0.931)
After pulse(fs)								
20.0	---	(0.856, 0.554)	---	(1.044, 0.516)	---	(0.780, 0.572)	---	(1.026, 0.516)
40.0	---	(0.950, 0.554)	---	(1.044, 0.516)	---	(0.610, 0.667)	---	(1.063 0.497)
60.0	---	(0.837, 0.572)	---	(1.082, 0.535)	---	(0.554, 0.875)	---	(1.044, 0.516)
80.0	---	(0.743, 0.591)	---	(0.818, 0.554)	---	(0.535, 1.082)	---	(1.044, 0.516)
100.0	---	(0.818, 0.572)	---	(0.705, 0.591)	---	(0.516, 1.063)	---	(1.082, 0.516)

4. Supplementary Materials S4. The variation of the precession $\mathbb{K}$, $\mathbb{K}'$ along the C1-C2 *BCP* bond-paths.
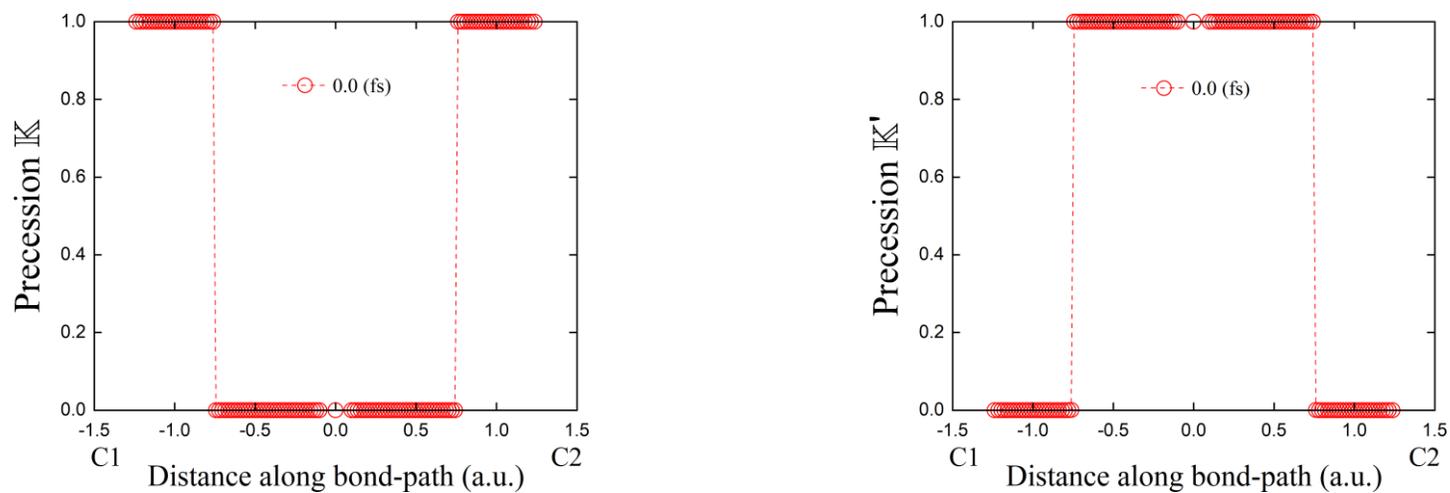

Figure S4(I). The variation of the precession $\mathbb{K}$, $\mathbb{K}'$ along the C1-C2 *BCP* bond-paths for $\mathbf{E}_x = 0$ au.

## 4. Supplementary Materials S4. Continued.
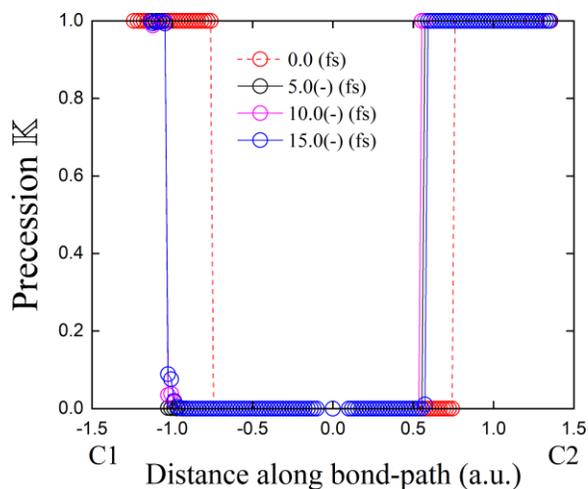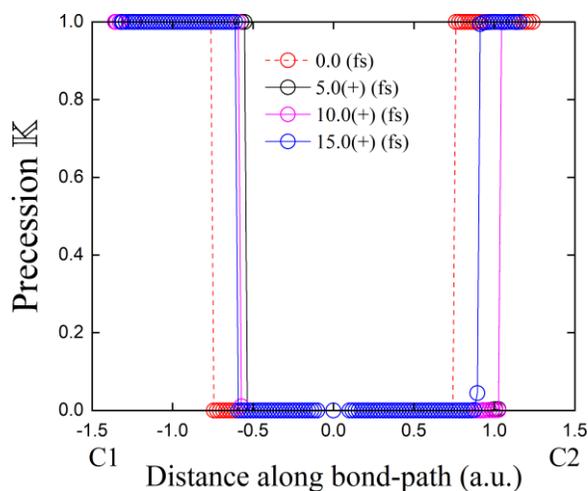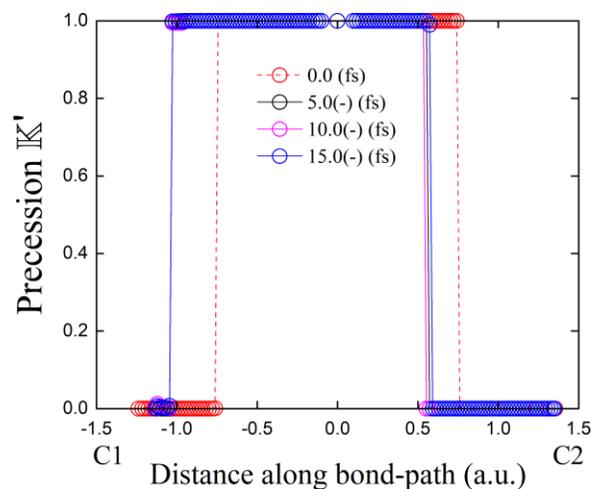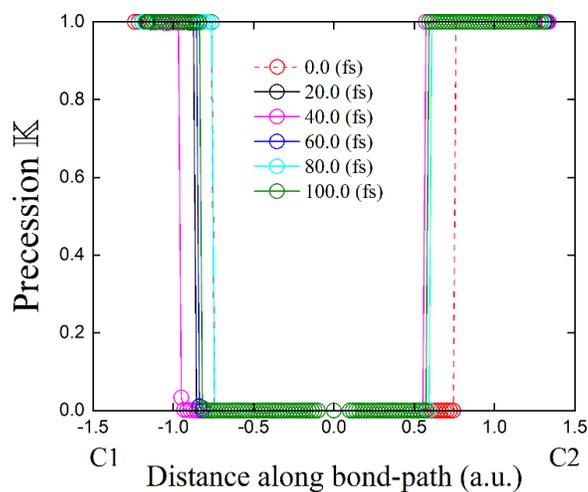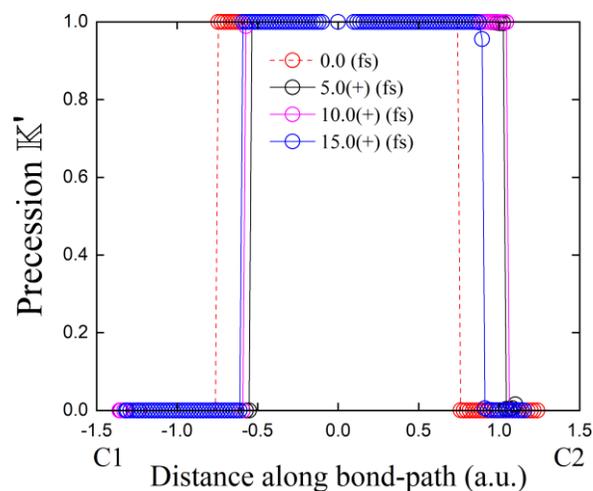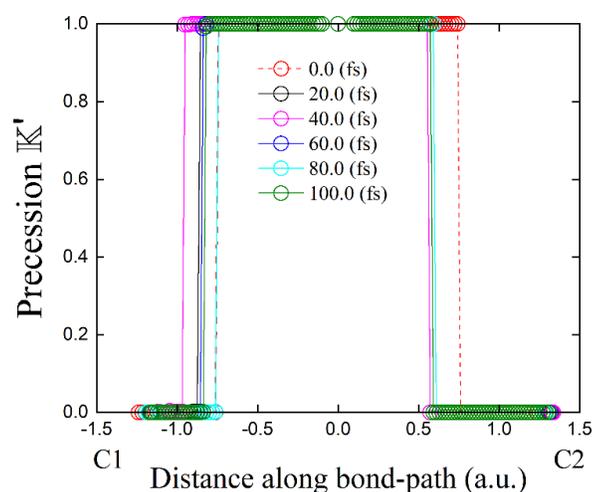
Figure S4(II). The variation of the precession $\mathbb{K}$, $\mathbb{K}'$ along the C1-C2 *BCP* bond-paths for $\omega = 0.2692$ au.

4. Supplementary Materials S4. Continued.
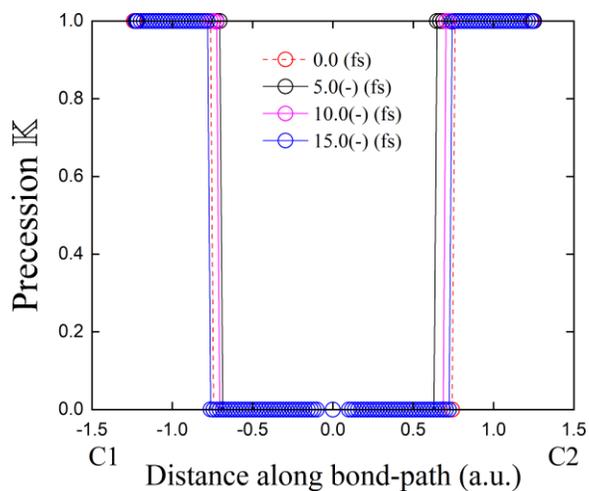
(a)
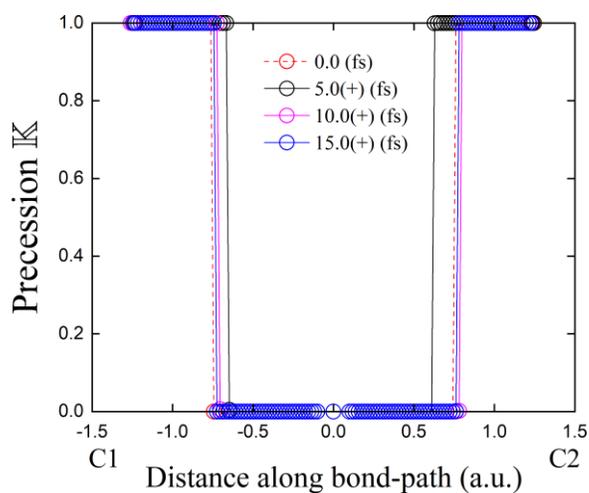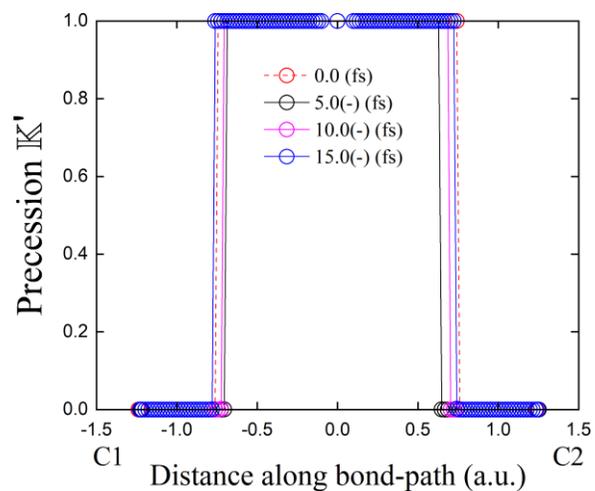
(b)
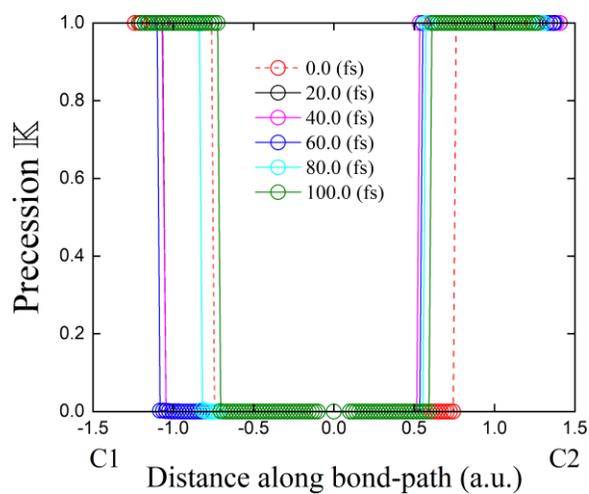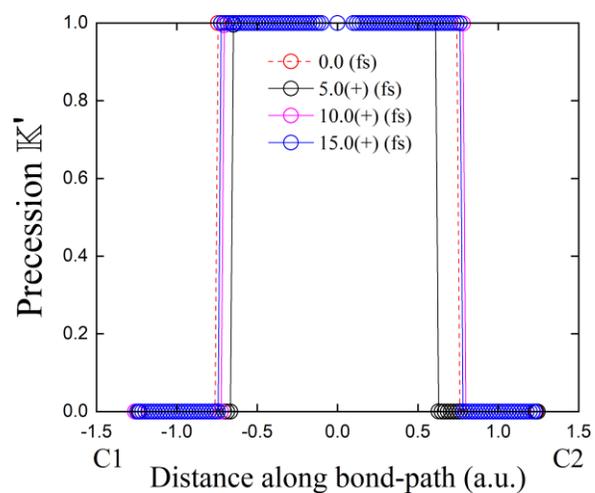
(c)
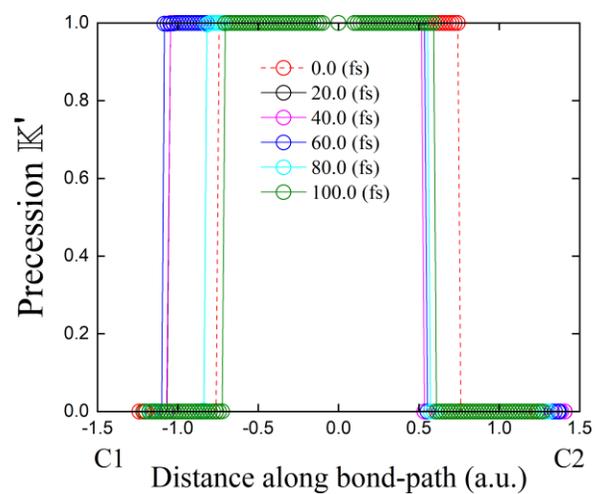
Figure S4(III). The variation of the precession $\mathbb{K}$, $\mathbb{K}'$ along the C1-C2 *BCP* bond-paths for $\omega = 0.2808$ au.

.

4. Supplementary Materials S4. Continued.
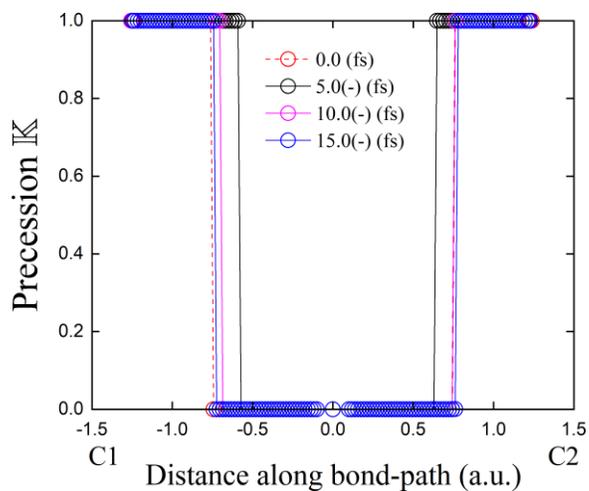
(a)
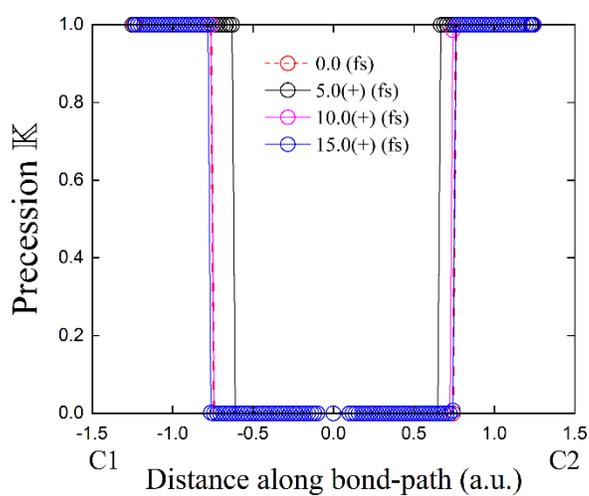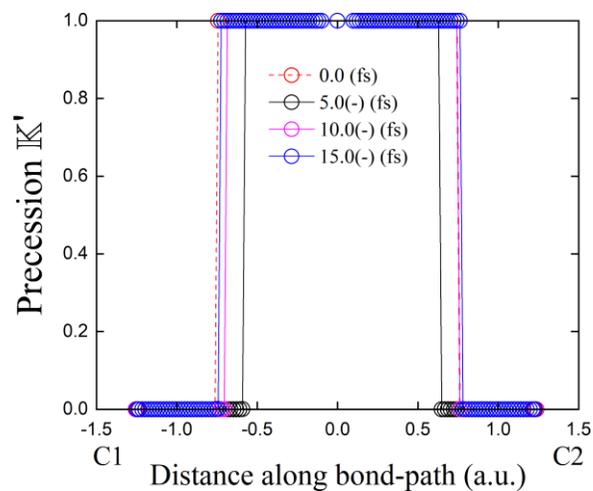
(b)
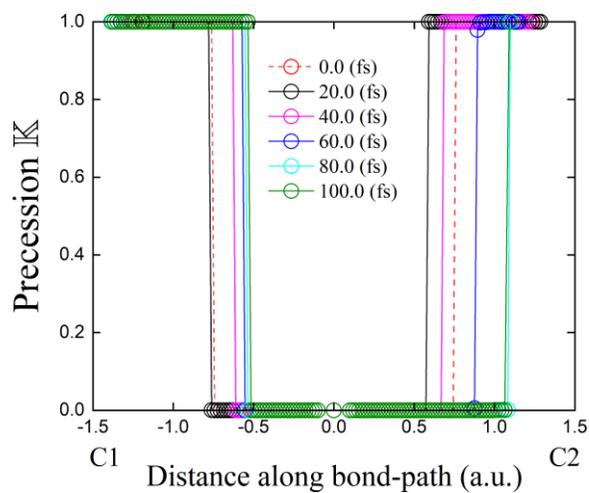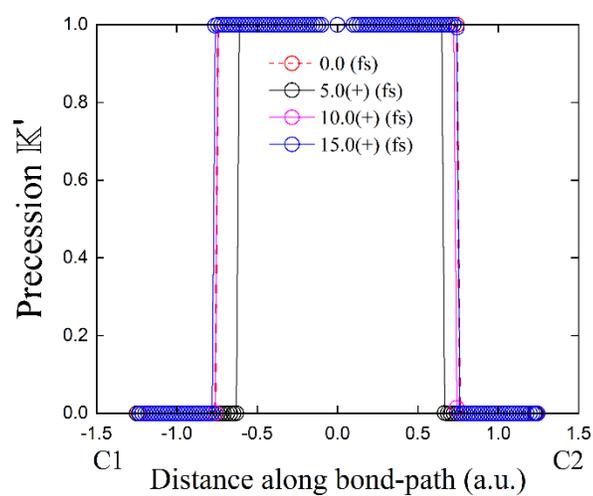
(c)
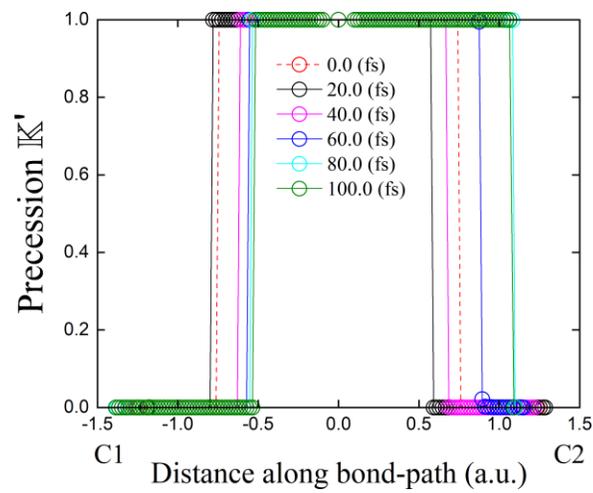
Figure S4(IV). The variation of the precession $\mathbb{K}$, $\mathbb{K}'$ along the C1-C2 *BCP* bond-paths for $\omega = 0.2830$ au.

.

4. Supplementary Materials S4. Continued.
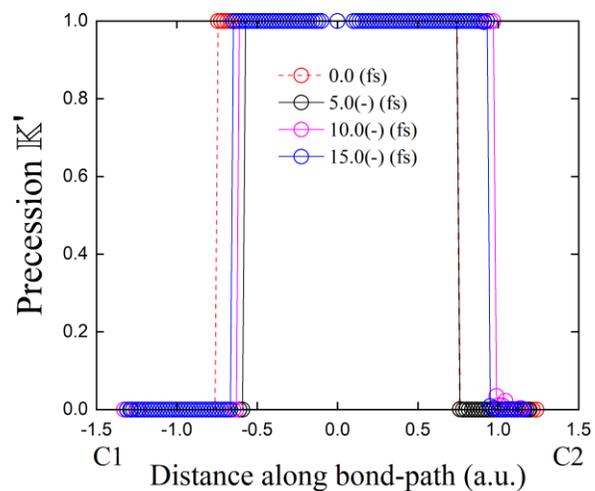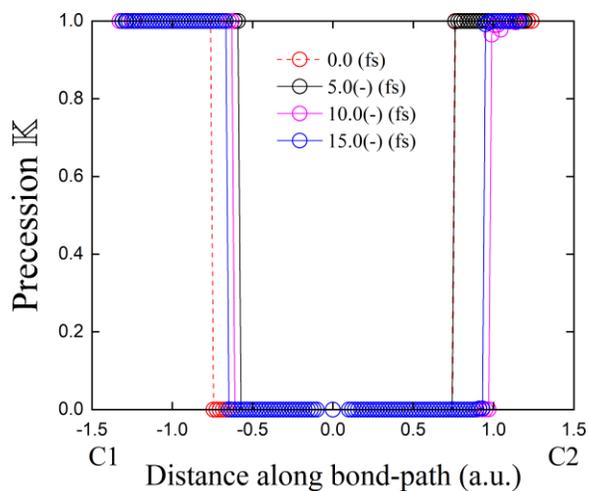
(a)
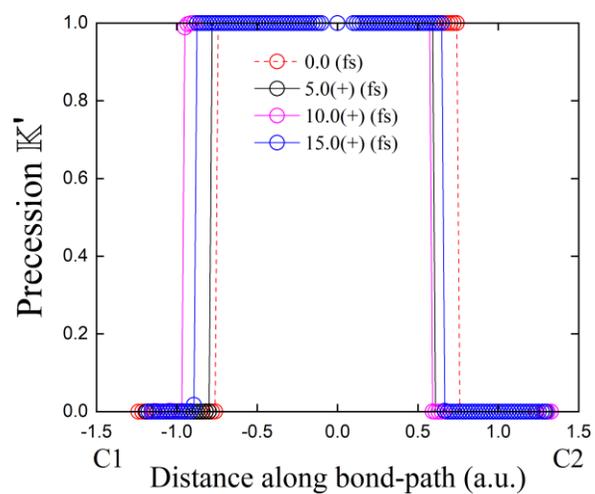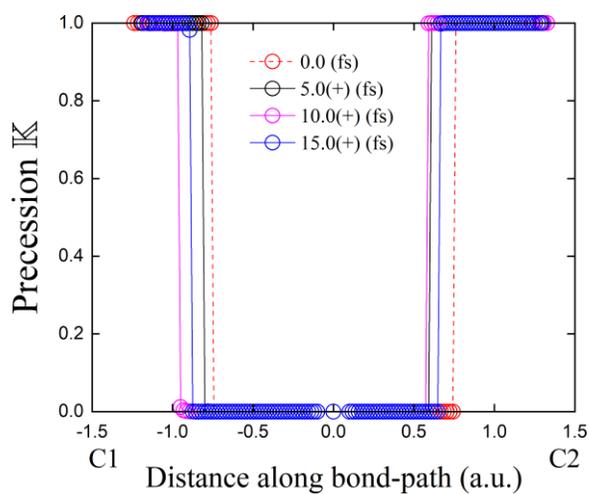
(b)
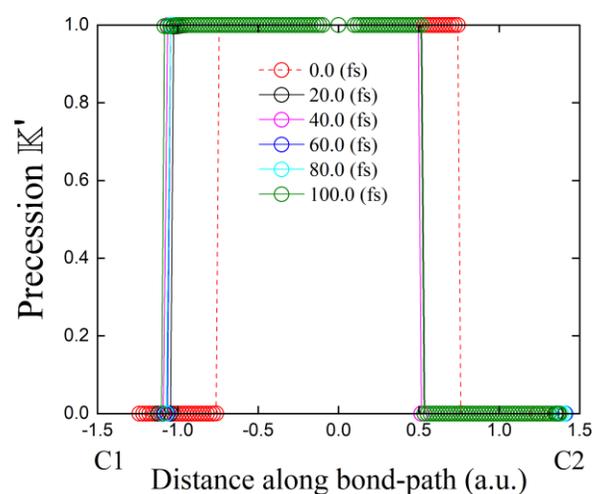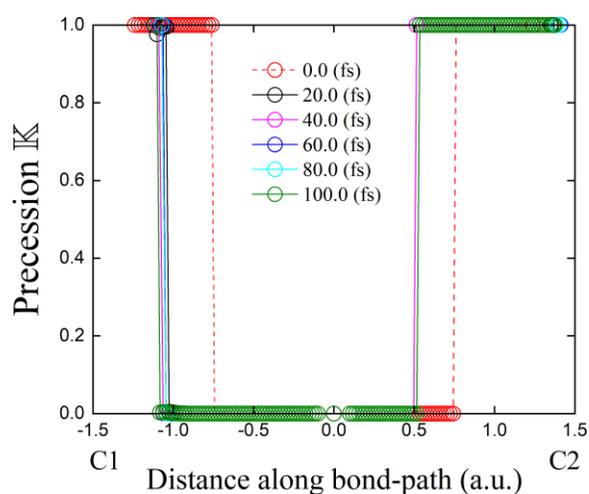
(c)

Figure S4(V). The variation of the precession $\mathbb{K}$, $\mathbb{K}'$ along the C1-C2 *BCP* bond-paths for $\omega = 0.290$ au.

.

5. Supplementary Materials S5. Ethene bond-path framework set $\mathbb{B}$ with $\{p, p'\}$ path-packets.

(a)

(b)

(c)
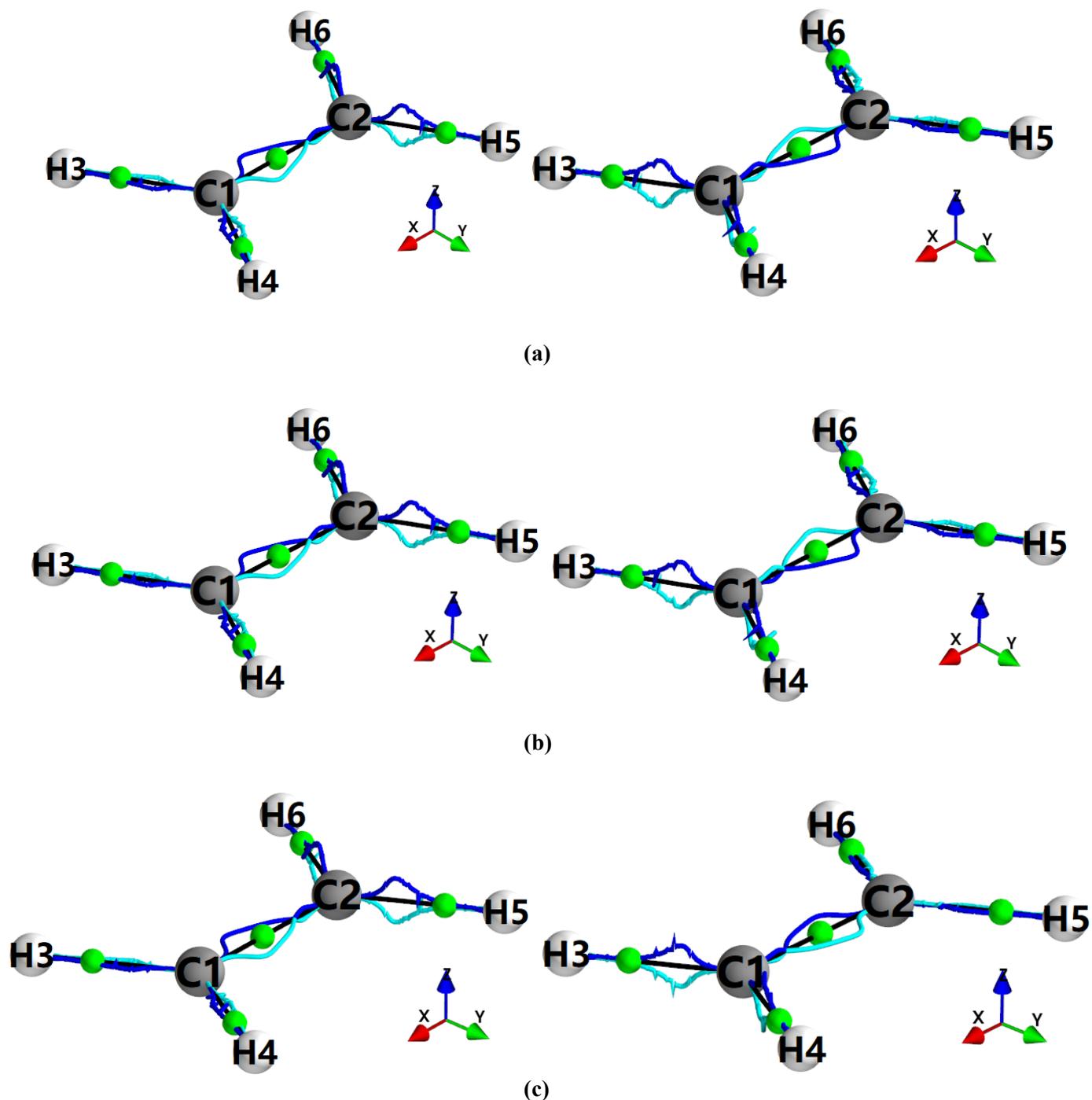
Figure S5(I). The ethene bond-path framework set $\mathbb{B}$ displaying the $\{p$ (blue), p' (cyan)$\}$ path-packets for values of the laser pulse frequency $\omega = 0.26917$ au for $\mathbf{E}_x = -98.2 \times 10^{-4}$ a.u at time = 4.944 femtoseconds (left-panel) and $\mathbf{E}_x = +107.0 \times 10^{-4}$ a.u. at time = 5.224 femtoseconds (right-panel) of sub-figure **(a)**. The $\{p,p'\}$ path-packets corresponding to the peak $\pm\mathbf{E}$-field values: $\mathbf{E}_x = -200.0 \times 10^{-4}$ a.u (at 10.022 fs) and $\mathbf{E}_x = +199.6 \times 10^{-4}$ a.u. (at 9.742 fs) are presented in the left and right panels respectively of sub-figure **(b)**. The $\{p,p'\}$ path-packets for $\mathbf{E}_x = -96.8 \times 10^{-4}$ a.u (at 15.101 fs) and $\mathbf{E}_x = +105.6 \times 10^{-4}$ a.u. (at 14.821 fs) are presented in the left and right panels respectively of sub-figure **(c)**. For further details see **Scheme 1.**

(a)

(b)

(c)

(d)

(e)
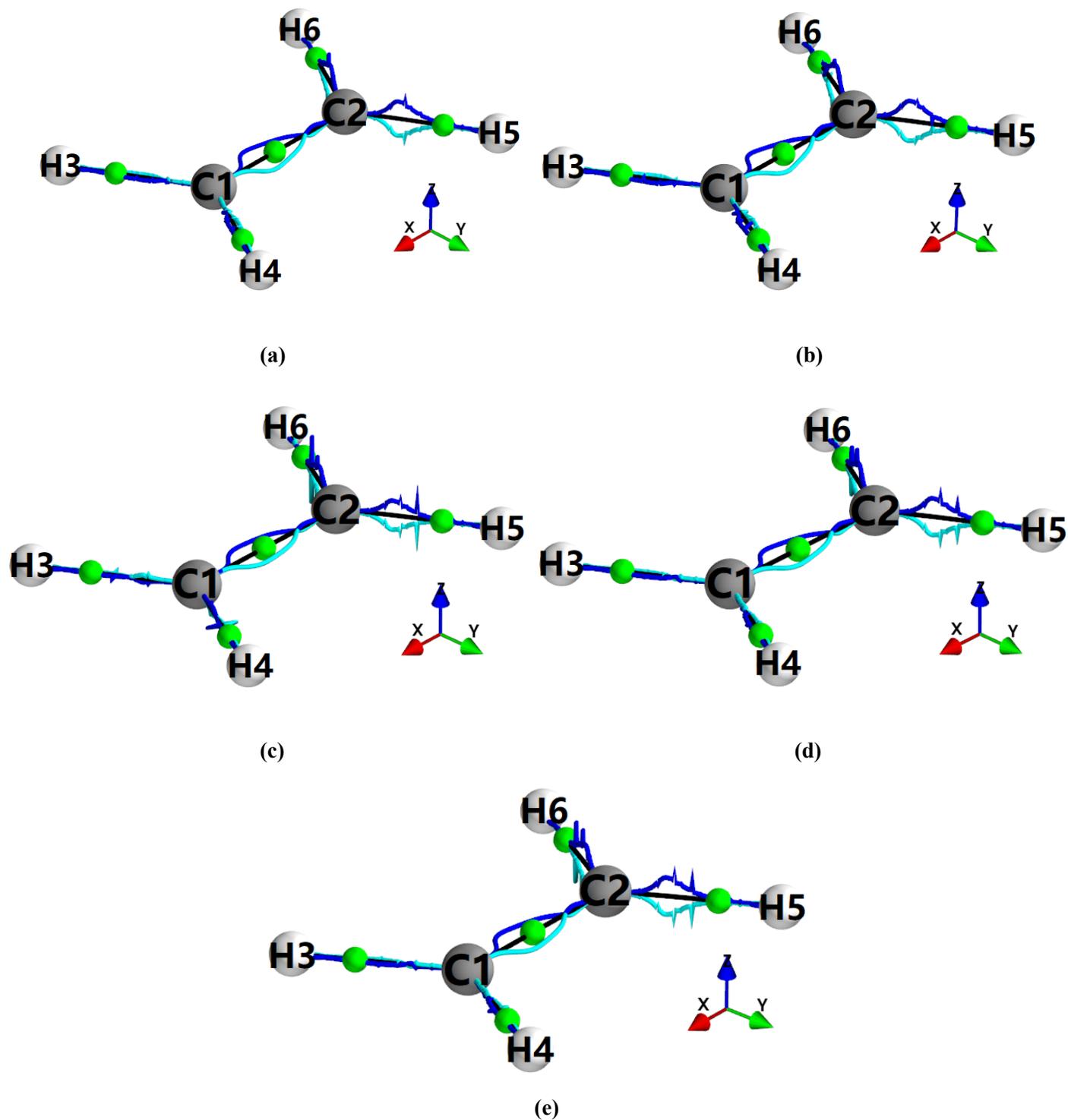
Figure S5(II). The ethene $\{p,p'\}$ path-packets for values of the laser pulse frequency $\omega = 0.26917$ au at the end of the pulse (20 fs), 40 fs, 60 fs, 80 fs and 100 fs are presented in sub-figures **(a)-(e)** respectively, see **Figure 1** for further details.

(a)

(b)

(c)
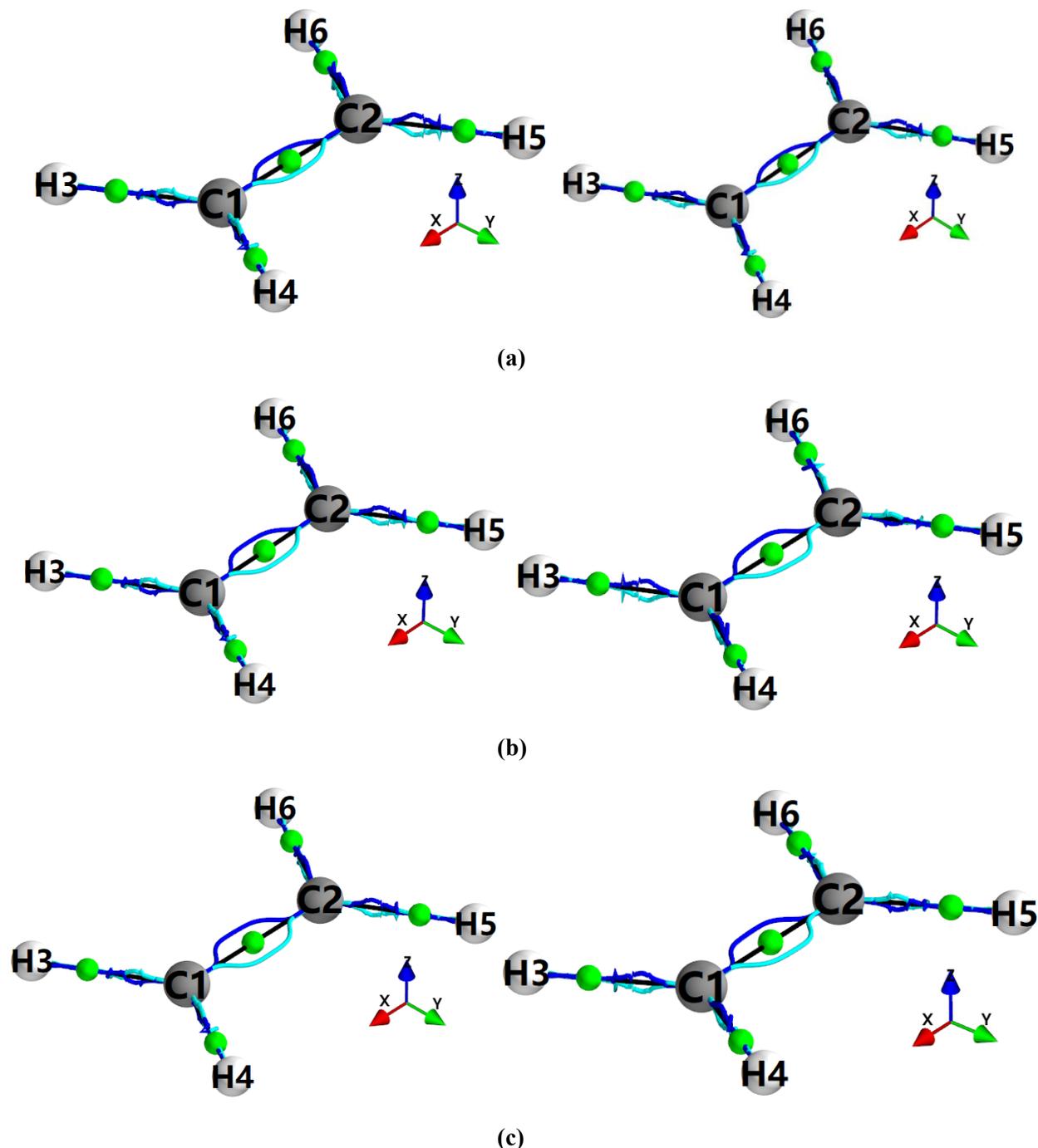
Figure S5(III). The ethene bond-path framework set $\mathbb{B}$ displaying the { p (blue), p' (cyan)} path-packets for values of the laser pulse frequency ω = 0.28081 au for $\mathbf{E}_x$ = -91.7×10^{-4} a.u at time = 4.741 femtoseconds (left-panel) and $\mathbf{E}_x$ = +100.2×10^{-4} a.u. at time = 5.011 femtoseconds (right-panel) of sub-figure **(a)**. The { p,p' } path-packets corresponding to the peak ±**E**-field values: $\mathbf{E}_x$ = -199.8×10^{-4} a.u (at 10.151 fs) and $\mathbf{E}_x$ = +199.7×10^{-4} a.u. (at 9.882 fs) are presented in the left and right panels respectively of sub-figure **(b)**. The {p,p'} path-packets for $\mathbf{E}_x$ = -99.3×10^{-4} a.u (at 15.022 fs) and $\mathbf{E}_x$ = +107.7×10^{-4} a.u. (at 14.752 fs) are presented in the left and right panels respectively of sub-figure **(c)**. For further details see **Scheme 1.**
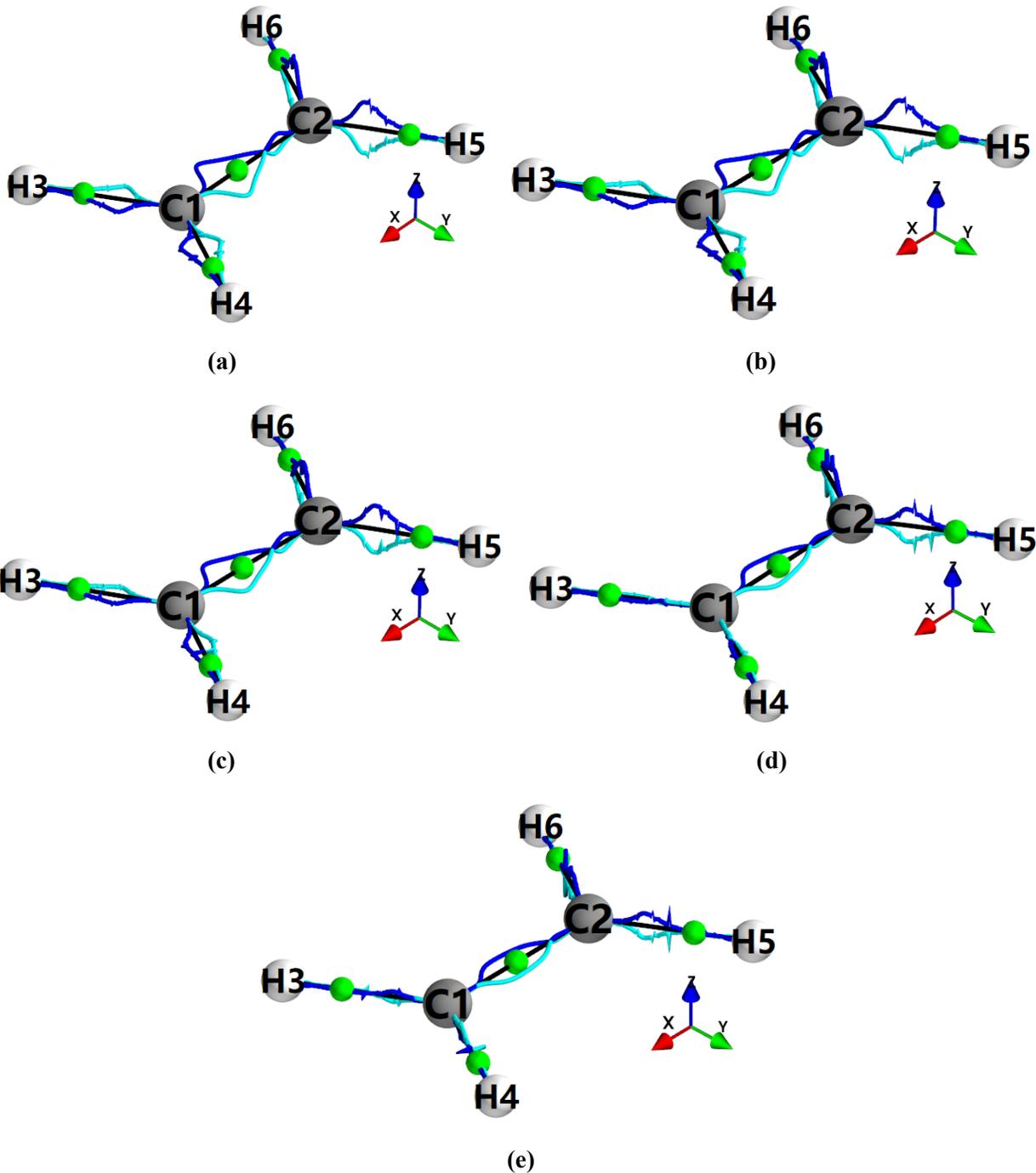
Figure S5(IV). The ethene $\{p,p'\}$ path-packets for values of the laser pulse frequency $\omega = 0.28081$ au at the end of the pulse (20 fs), 40 fs, 60 fs, 80 fs and 100 fs are presented in sub-figures **(a)-(e)** respectively, see **Figure 2** for further details.
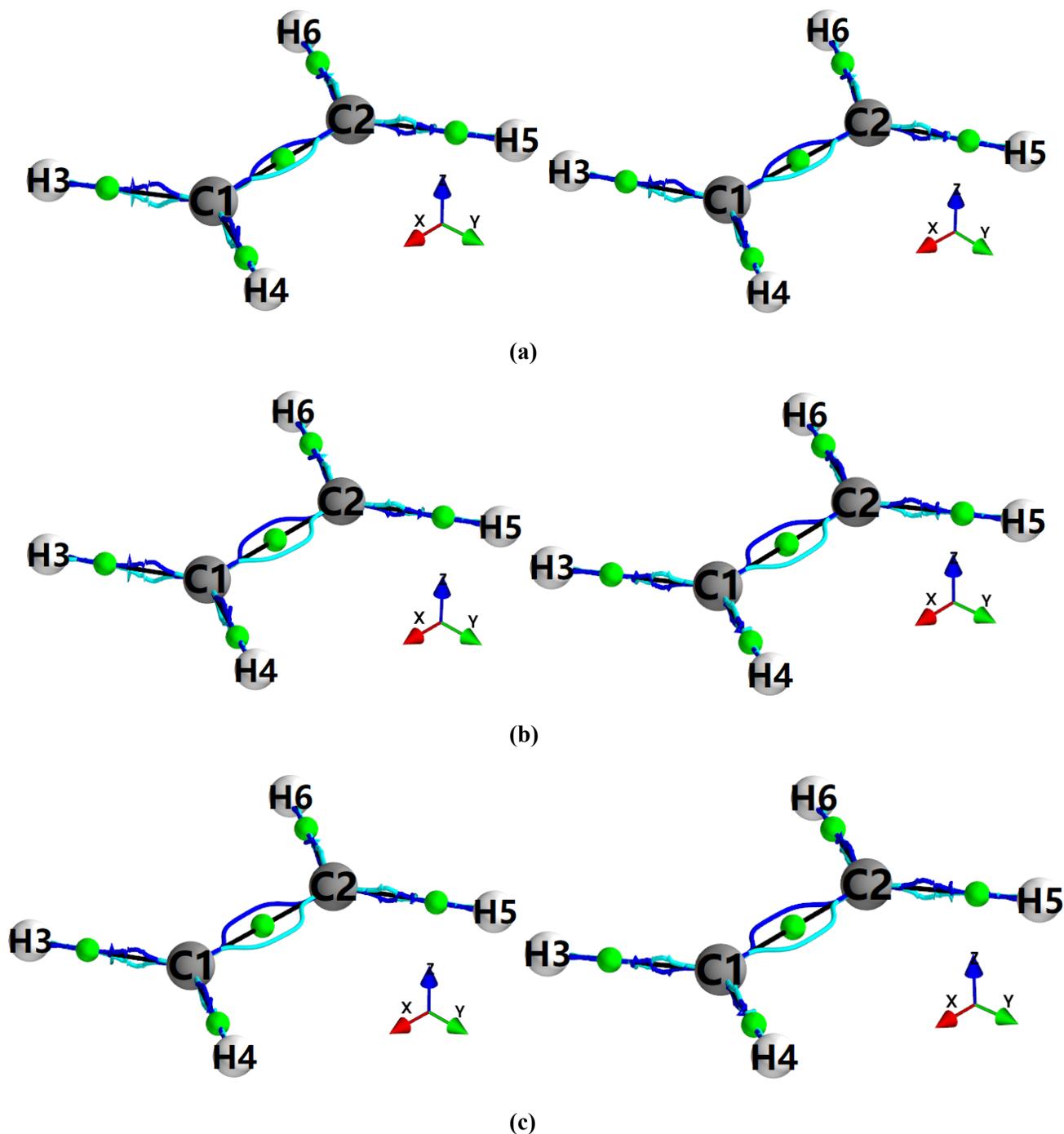
Figure S5(V). The ethene bond-path framework set $\mathbb{B}$ displaying the { p (blue), p' (cyan)} path-packets for values of the laser pulse frequency $\omega = 0.283$ au for $\mathbf{E}_x = -107.4 \times 10^{-4}$ a.u at time = 5.235 femtoseconds (left-panel) and $\mathbf{E}_x = +99.0 \times 10^{-4}$ a.u. at time = 4.968 femtoseconds (right-panel) of sub-figure **(a)**. The { p,p' } path-packets corresponding to the peak $\pm\mathbf{E}$-field values: $\mathbf{E}_x = -199.6 \times 10^{-4}$ a.u (at 10.064 fs) and $\mathbf{E}_x = +199.6 \times 10^{-4}$ a.u. (at 9.797 fs) are presented in the left and right panels respectively of sub-figure **(b)**. The {p,p'} path-packets for $\mathbf{E}_x = -103.0 \times 10^{-4}$ a.u (at 14.904 fs) and $\mathbf{E}_x = +94.6 \times 10^{-4}$ a.u. (at 15.171 fs) are presented in the left and right panels respectively of sub-figure **(c)**. For further details see **Scheme 1.**

(a)

(b)


(c)

(d)

(e)
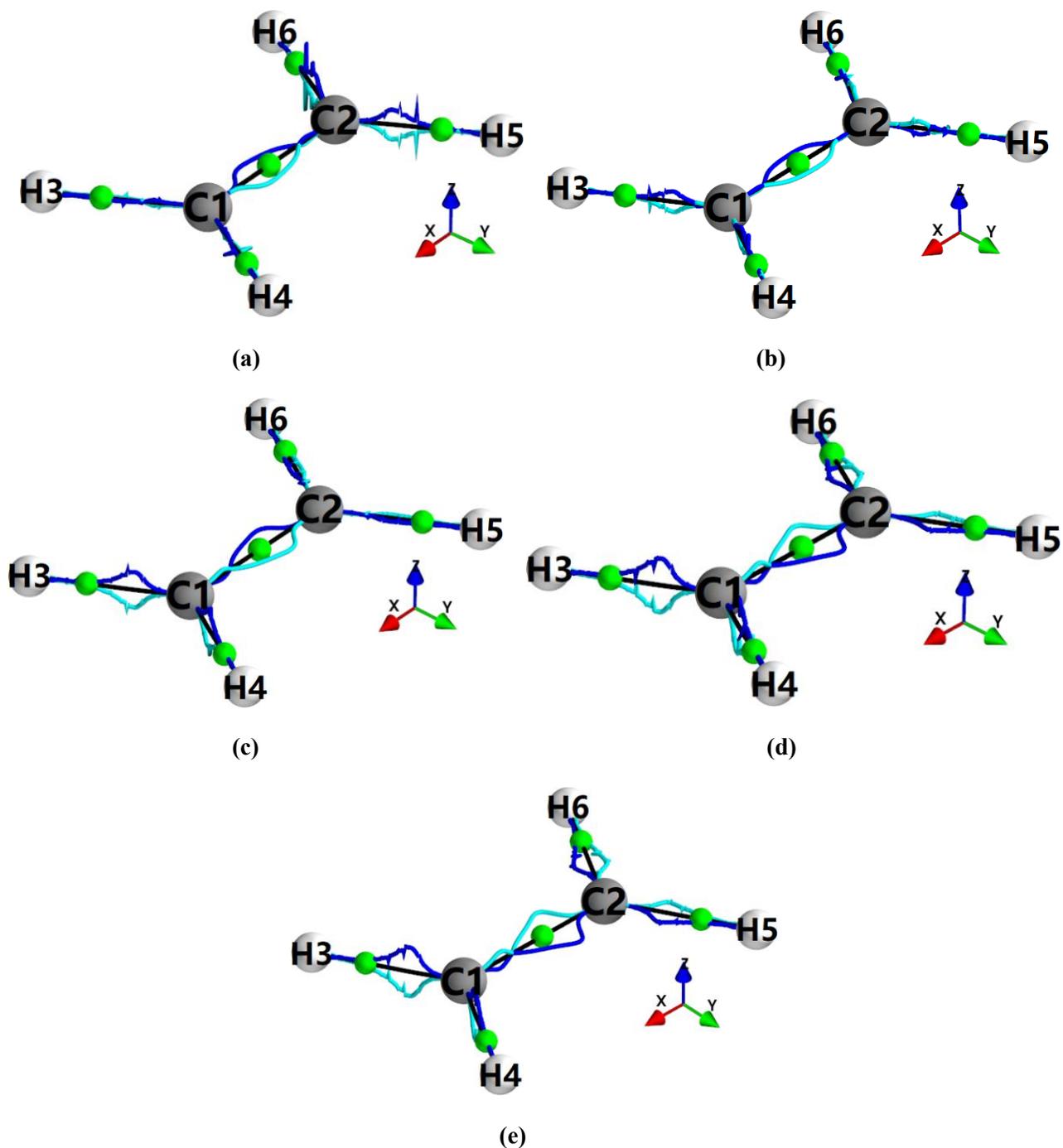
Figure S5(VI). The ethene $\{p,p'\}$ path-packets for values of the laser pulse frequency $\omega = 0.283$ au at the end of the pulse (20 fs), 40 fs, 60 fs, 80 fs and 100 fs are presented in sub-figures **(a)-(e)** respectively, see **Figure 3** for further details.
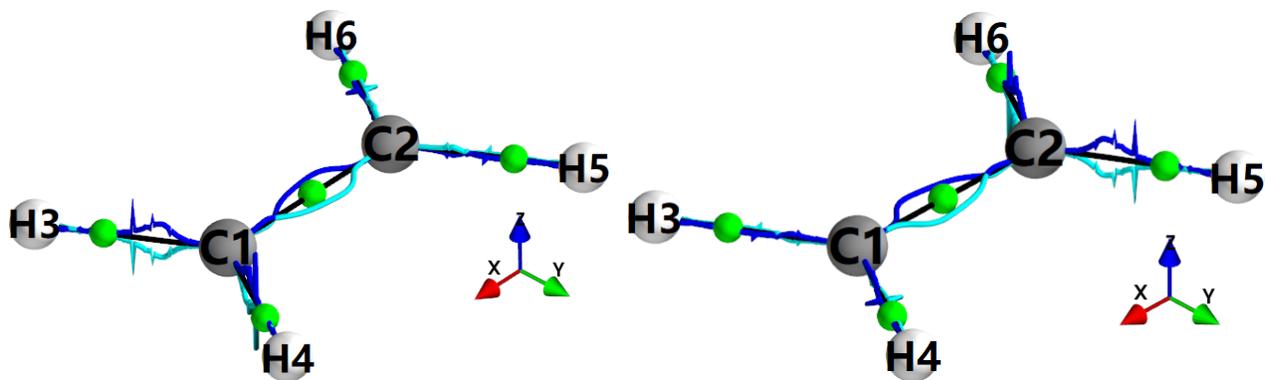
(a)
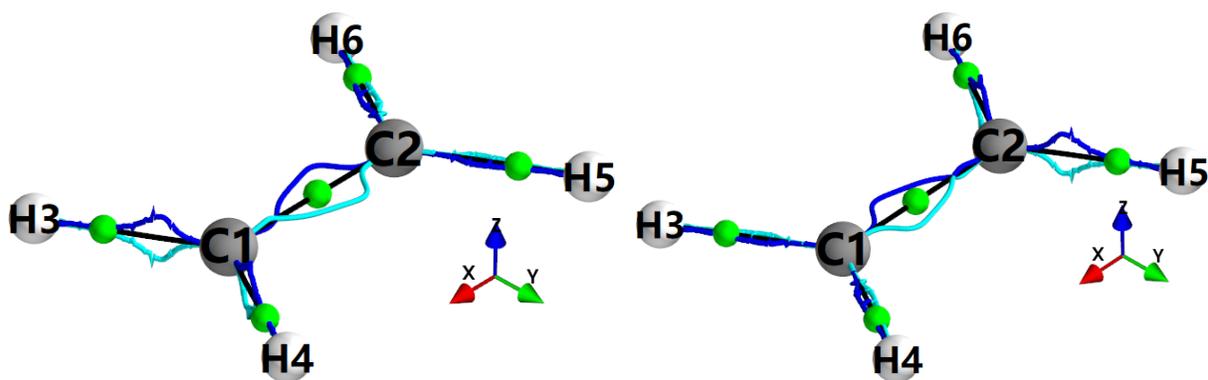
(b)
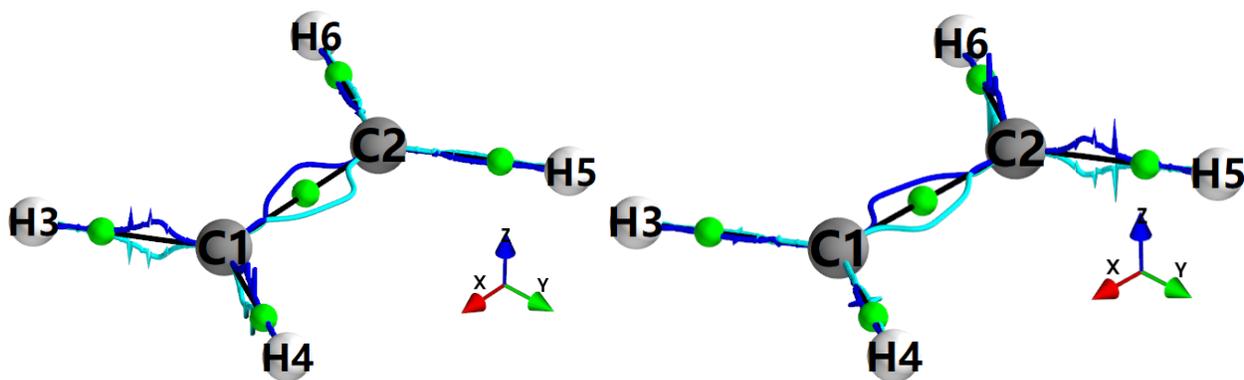
(c)

Figure S5(VII). The ethene bond-path framework set $\mathbb{B}$ displaying the {*p* (blue), *p′* (cyan)} path-packets for values of the laser pulse frequency ω = 0.290 au for $\mathbf{E}_x$ = -103.4×10^{-4} a.u at time = 5.115 femtoseconds (left-panel) and $\mathbf{E}_x$ = +95.1×10^{-4} a.u. at time = 4.854 femtoseconds (right-panel) of sub-figure **(a)**. The {*p,p′*} path-packets corresponding to the peak ±E-field values: $\mathbf{E}_x$ = -199.7×10^{-4} a.u (at 9.823 fs) and $\mathbf{E}_x$ = +199.6×10^{-4} a.u. (at 10.083 fs) are presented in the left and right panels respectively of sub-figure **(b)**. The {*p,p′*} path-packets for $\mathbf{E}_x$ = -97.9×10^{-4} a.u (at 15.062 fs) and $\mathbf{E}_x$ = +106.1×10^{-4} a.u. (at 14.802 fs) are presented in the left and right panels respectively of sub-figure **(c)**. For further details see **scheme 1.**

(a)

(b)

(c)

(d)

(e)
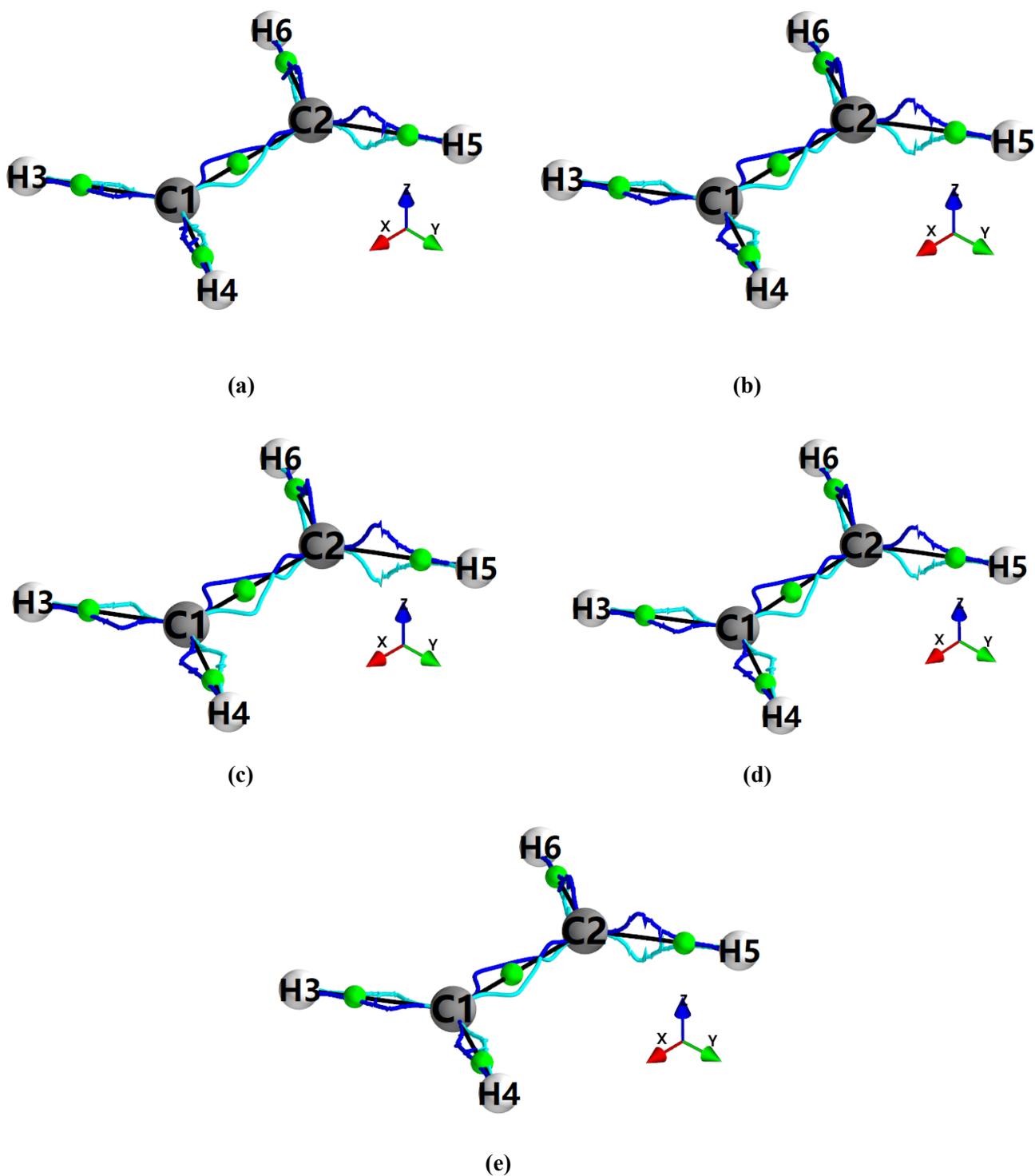
Figure S5(VIII). The ethene $\{p,p'\}$ path-packets for values of the laser pulse frequency $\omega = 0.290$ au after the pulse (20 fs), 40 fs, 60 fs, 80 fs and 100 fs are presented in sub-figures **(a)-(e)** respectively, see **Figure 4** for further details.
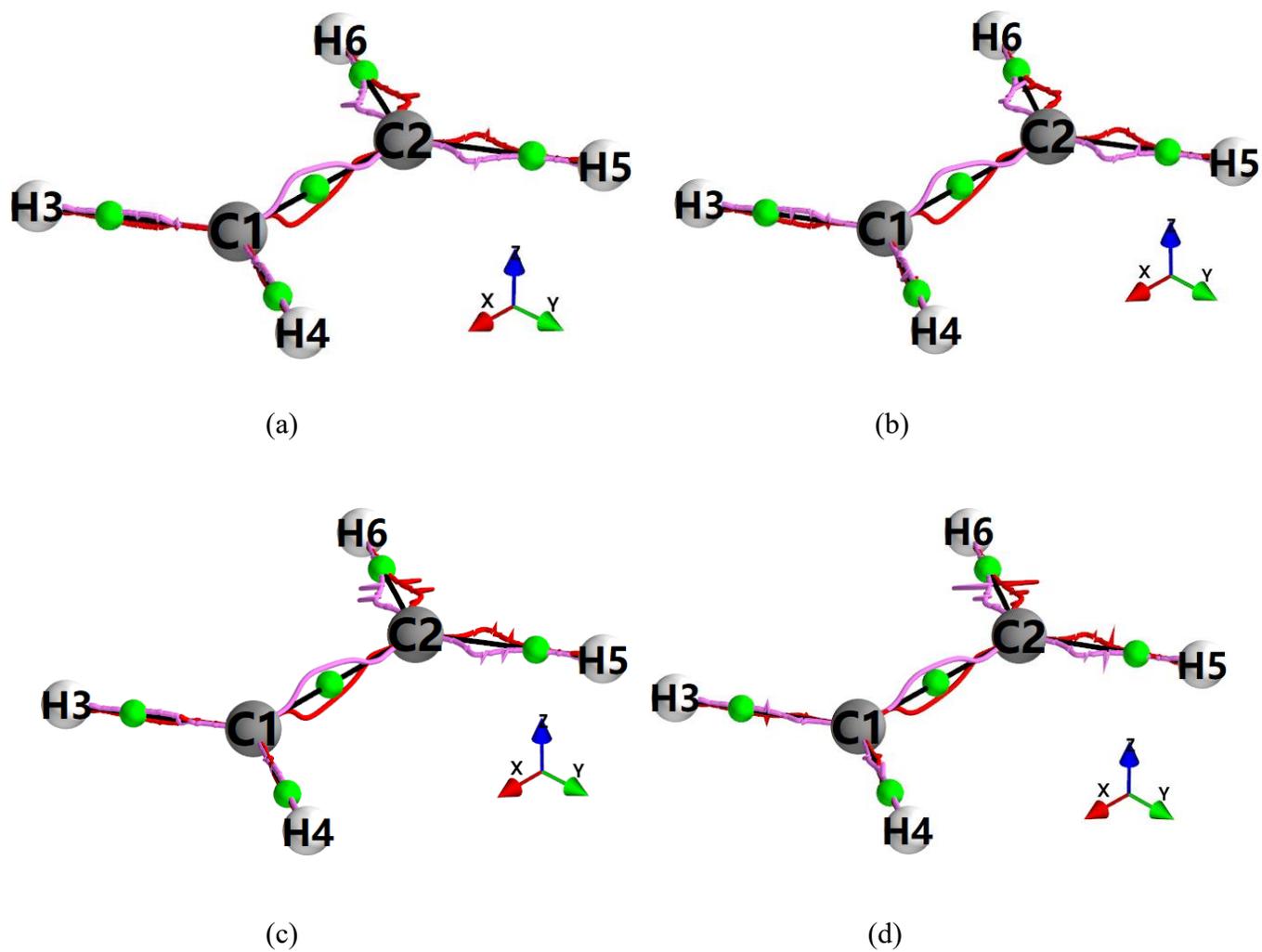
Figure S5(IX). The ethene $\{q,q'\}$ path-packets for values of the laser pulse frequency $\omega = 0.26917$ au after the pulse (20 fs), 40 fs, 60 fs and 80 fs are presented in sub-figures **(a)-(d)** respectively, see **Figure 1** for further details.
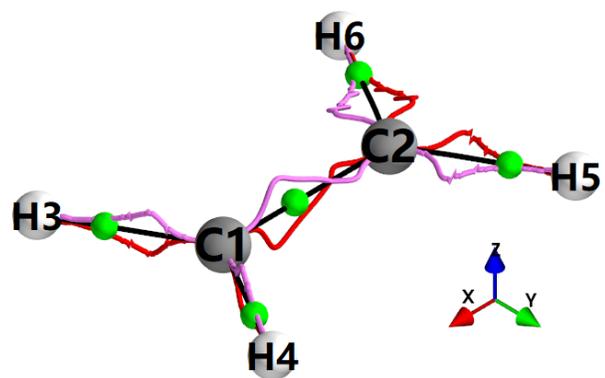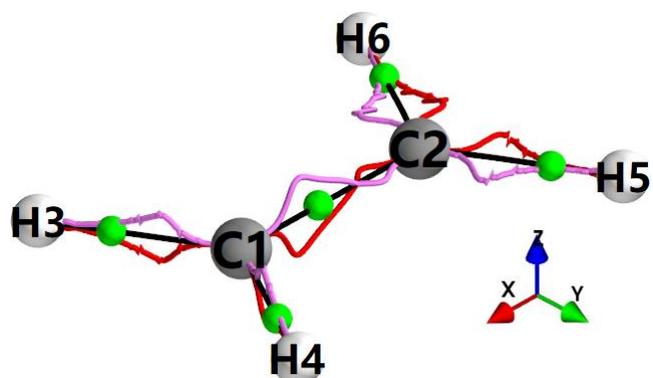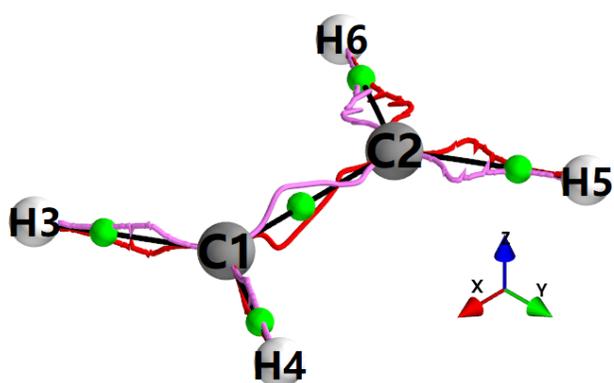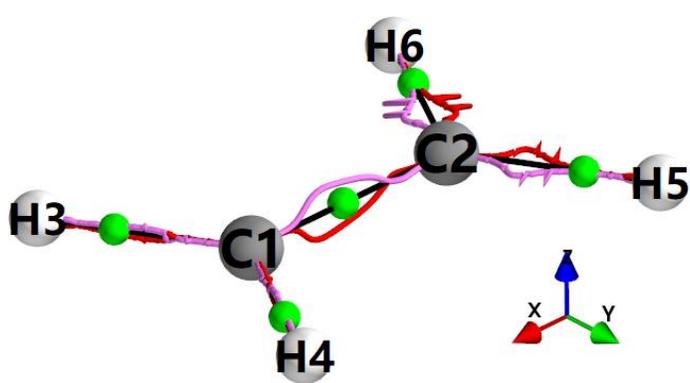
Figure S5(X). The ethene $\{q,q'\}$ path-packets for values of the laser pulse frequency $\omega = 0.28081$ au after the pulse (20 fs), 40 fs, 60 fs and 80 fs are presented in sub-figures **(a)-(d)** respectively, see **Figure 2** for further details.
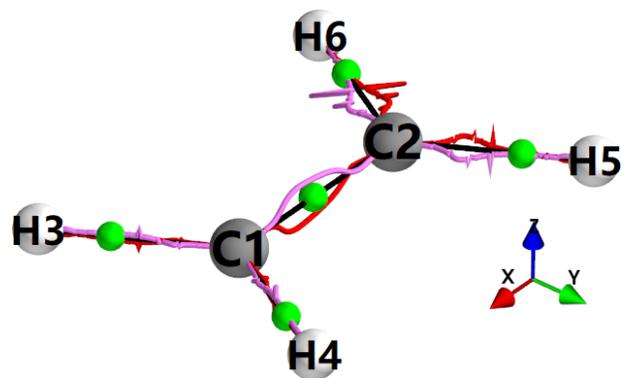
(a)
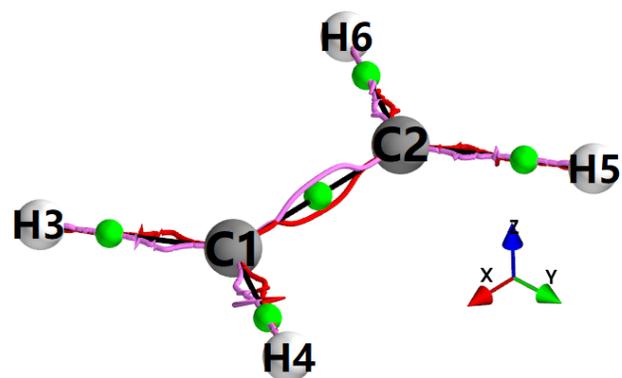
(b)
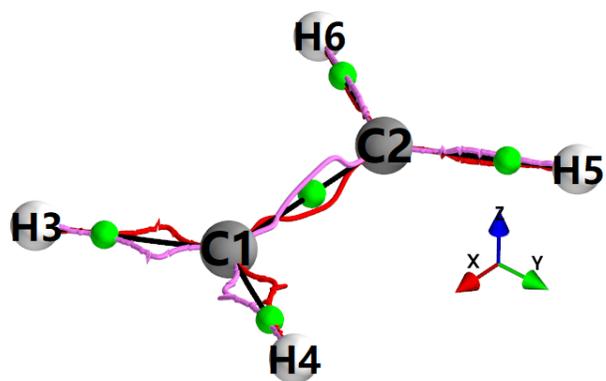
(c)
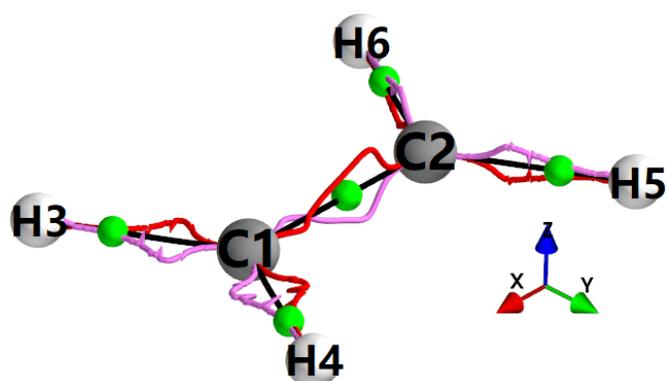
(d)

Figure S5(XI). The ethene $\{q,q'\}$ path-packets for values of the laser pulse frequency $\omega = 0.283$ au after the pulse (20 fs), 40 fs, 60 fs and 80 fs are presented in sub-figures **(a)-(d)** respectively, see **Figure 3** for further details.
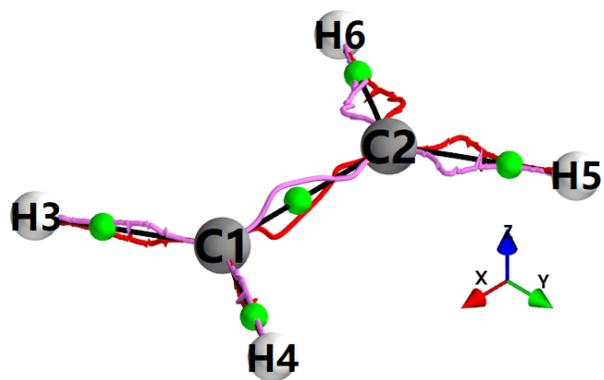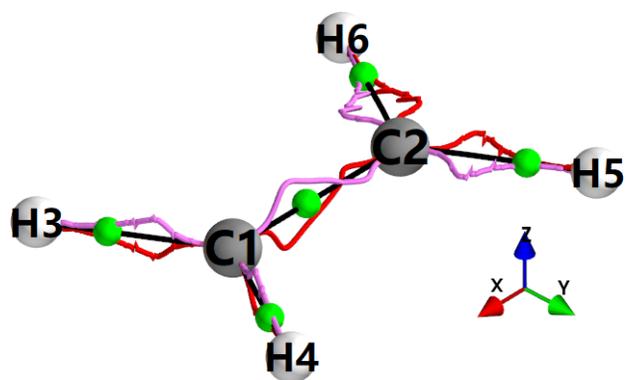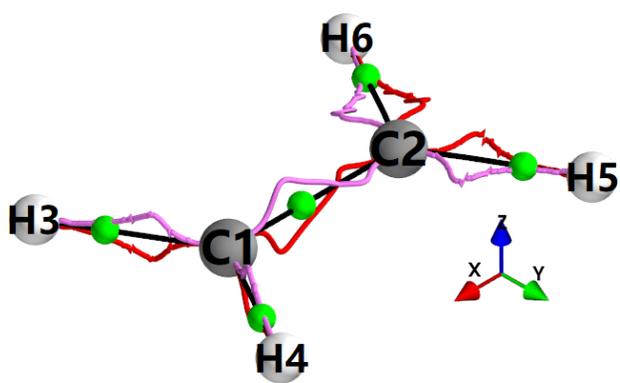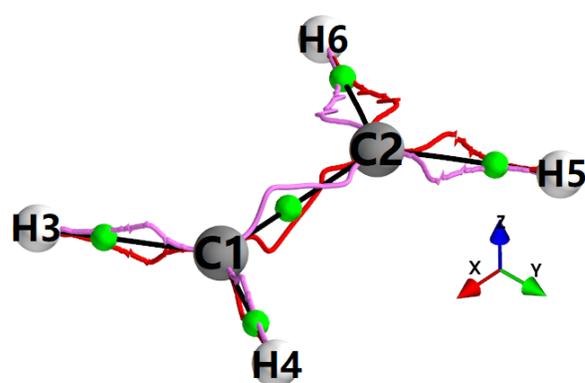
Figure S5(XII). The ethene $\{q, q'\}$ path-packets for values of the laser pulse frequency $\omega = 0.290$ au after the pulse (20 fs), 40 fs, 60 fs and 80 fs are presented in sub-figures **(a)-(d)** respectively, see **Figure 4** for further details.